Scientific Research Publishing

Smart Grid and Renewable Energy, 2023, 14, 209-220
https://www.scirp.org/journal/sgre
ISSN Online: 2151-4844
ISSN Print: 2151-481X

Investigation of the Behavior of a Photovoltaic Cell under Concentration as a Function of the Temperature of the Base and a Variable External Magnetic Field in 3D Approximation

Boubacar Soro[1,2*], Adama Ouedraogo[1,3], Mahamadi Savadogo[1], Ramatou Konate[1], Guyserge Tchouadep[1], Martial Zoungrana[1], Sié Kam[1]

[1]Laboratory of Thermal and Renewable Energies, Department of Physics, Université Joseph Ki-Zerbo, Ouagadougou, Burkina Faso
[2]Institutdes Sciences et Technologie, Ecole Normale Supérieure, Ouagadougou, Burkina Faso
[3]Centre Universitaire Polytechnique de Kaya, Université Joseph Ki-Zerbo, Ouagadougou, Burkina Faso
Email: *soro.bo@gmail.com

How to cite this paper: Soro, B., Ouedraogo, A., Savadogo, M., Konate, R., Tchouadep, G., Zoungrana, M. and Kam, S. (2023) Investigation of the Behavior of a Photovoltaic Cell under Concentration as a Function of the Temperature of the Base and a Variable External Magnetic Field in 3D Approximation. *Smart Grid and Renewable Energy*, **14**, 209-220.
https://doi.org/10.4236/sgre.2023.1412013

Received: October 31, 2023
Accepted: December 25, 2023
Published: December 28, 2023

Abstract

The photovoltaic (PV) cell performances are connected to the base photogenerated carriers charge. Some studies showed that the quantity of the photogenerated carriers charge increases with the increase of the solar illumination. This situation explains the choice of concentration PV cell ($C = 50$ suns) in this study. However, the strong photogeneration of the carriers charge causes a high heat production by thermalization, collision and carriers charge braking due to the electric field induced by concentration gradient. This heat brings the heating of the PV cell base. That imposes the taking into account of the temperature influence in the concentrator PV cell operation. Moreover, with the proliferation of the magnetic field sources in the life space, it is important to consider its effect on the PV cell performances. Thus, when magnetic field and base temperature increase simultaneously, we observe a deterioration of the photovoltage, the electric power, the space charge region capacity, the fill factor and the conversion efficiency. However the photocurrent increases when the base temperature increases and the magnetic field strength decreases. It appears an inversion phenomenon in the evolution of the electrical parameters as a function of magnetic field for the values of magnetic field $B > 4\times10^{-4}$ T.

Keywords

Thermalization, Base Temperature, Magnetic Field, Fill Factor, Efficiency,

Space Charge Region Capacity

1. Introduction

The performances of a PV cell are dependent on external factors, such as solar radiation, temperature, gamma radiation, etc. Indeed, in the presence of gamma radiation, the performances of a PV cell could degrade [1]. The same is true for operating a PV cell in a high heat environment, resulting in a rise in its temperature. The rise of temperature can come from the activities in the cell or from exposure under the sun, through the radiant light. Whatever the source of temperature rise, it contributes to reducing the proper functioning of a PV cell [2]. On the other hand, the increase in illumination produces an improvement in the performances of a PV cell. Note that the photovoltaic market is dominated by silicon PV cells [3]. However, the laboratory conversion efficiency of a silicon PV cell single junction is only about 26.8%, under non illumination concentration [3]. This efficiency seems low given the growth in energy demand. Consequently, research has turned to other materials such as thin films and organic semiconductors. Other research work has also focused on concentrated polycrystalline silicon PV cells. For a concentrated PV cell, given the illumination mode, the number of photogenerated charge carriers in the base is very high. The concentrated PV cell has the advantage of having better efficiency than the non-concentrated one, up to 27.6% in the laboratory [2], using less material thanks to its reduced size and occupying less space. The inconvenience of concentrating PV cells is that they produce a lot of heat during operation, causing high temperature. Indeed, the variations of the photocurrent and the photovoltage are coming from internal factors related to the movements of the charge carriers and which affect the temperature of the base [4] [5]. In addition, the multiplicity of magnetic field sources in our living environment (telecommunication antennas, transformers, TV and radio antennas, etc.) causes a magnetic influence on the PV cells during their operation. Indeed, the magnetic field, through the Lorentz force, acts on the movement of charge carriers by modifying their trajectory. Consequently, the presence of magnetic field influences the performance of PV cells [6] [7]. It is therefore instructive to investigate the cumulative influence of residual heat due to the movement of charge carriers and the magnetic field on the behaviour of a concentrated PV cell in order to contribute to the deployment of this technology in Sahel region. Thus, this study presents the combined effects of base heating and a variable external magnetic field on the operation of a concentration PV cell. After the introduction, the methods and theories, the hypotheses and the mathematical model used will be discussed afterwards. Finally, the results and discussion on the simultaneous influence of heat and magnetic field on the electrical parameters of a concentrated PV cell will be presented. This work will end with a conclusion and recommen-

dations.

2. Methods and Theories

2.1. Mathematical Modulization and Assumptions

In this study, the polycrystalline silicon PV cell used is formed by a lot of grains with different sizes. All the grains are assumed cubic [8] [9]. That leads to finding the real physical situation with the consideration of the grain boundaries recombination velocity. Figure 1 illustrates the cubic grain.

Each grain presents the sizes g_x following (ox) axis and g_y following (oy) axis. In cubic grain $g_x = g_y$ and H gives the PV cell base depth following (oz) axis. Recombination planes are the adjacent g_x surfaces of two grains and are located at positions $x = \pm\frac{g_x}{2}$ and $y = \pm\frac{g_y}{2}$ respectively perpendicular. These planes are perpendicular to (ox) and (oy) axes of the coordinate system [9] [10]. In this model, the magnetic field is applied along the direction of the (oy) axis, *i.e.* parallel to the junction and by this assumption the base doping rate is uniform. This leads to an almost zero crystalline electric field.

Moreover, the rate of absorption of light being a function of the depth z ($0 \le z \le H$) of the base, there is thus a non-uniform generation of the charge carriers in the volume of the base. The concentration of charge carriers is then high in the regions close to the illuminated surface and then decreases as moving away from this surface. This variation in charge carrier density along the oz axis is the source of an internal electric field $E(z)$ called the concentration gradient electric field of excess minority carriers [6] [11]. This electric field will have an influence on the mobility of the charge carriers in the volume of the base. Light enters the PV cell along the oz axis. This leads to a generation of charge carriers along this same axis. By assumption, the charge carrier density is uniform along the ox and oy axes. The concentration gradient electric field is therefore zero along these two axes: $E(x) = E(y) = 0$.

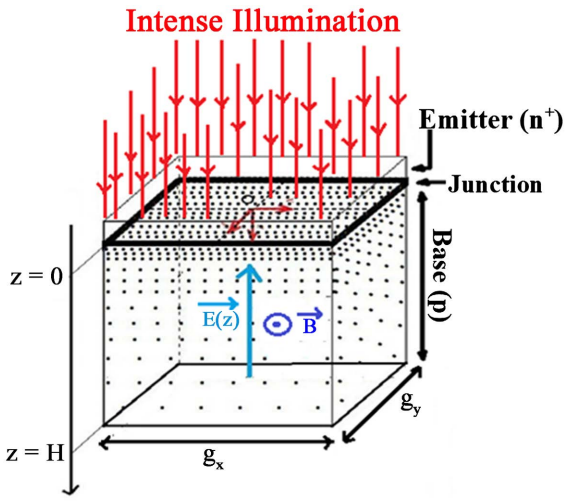

Figure 1. PV cell cubic grain under concentrated illumination and under magnetic field.

The grain is also subjected to a variable magnetic field $\boldsymbol{B}$ oriented along the (oy) axis as shown in **Figure 1** above. By assumption, the PV cell is under a static illumination regime.

2.2. Mathematical Modulization

The magneto-transport equation in the base of the PV cell under an intense multi-spectral illumination and under a variable magnetic field, is given by the following relationship [12].

$$\boldsymbol{J}_n = eD_n \nabla \delta(x,y,z) + e\mu_n \delta(x,y,z)\boldsymbol{E}(z) - \mu_n \boldsymbol{J}_n \wedge B \tag{1}$$

D_n and D_p being respectively the diffusion coefficients of electrons and holes in the base of the PV cell; μ_n and μ_p are respectively the mobilities of electrons and holes in the base of the silicon PV cell. The mobilities of electrons and holes depend on the absolute temperature T of the base of the PV cell and are given by the following expressions [5]:

$$\mu_n(T) = \mu_{on}\left(\frac{T}{T_0}\right)^{-1.5} \tag{2}$$

and

$$\mu_p(T) = \mu_{op}\left(\frac{T}{T_0}\right)^{-1.5} \tag{3}$$

With $\mu_{on} = 1500\ \mathrm{cm}^2 \cdot \mathrm{V}^{-1} \cdot \mathrm{s}^{-1}$ and $\mu_{on} = 475\ \mathrm{cm}^2 \cdot \mathrm{V}^{-1} \cdot \mathrm{s}^{-1}$ at $T_0 = 300\ \mathrm{K}$. As the diffusion coefficient depends on the mobility of the carriers which causes the heating of the base, the diffusion coefficients of electrons and holes consequently depend on the temperature T of the base of the PV cell and are expressed as follows [5]:

$$D_n(T) = \frac{K_B \cdot T}{q}\mu_n(T) \tag{4}$$

and

$$D_p(T) = \frac{K_B \cdot T}{q}\mu_p(T) \tag{5}$$

k_B is the Boltzmann constant and q the elementary electric charge. The illumination being intense, the expression of the crystalline electric field due to the concentration gradient is given by [11]:

$$E(z) = \frac{D_p(T) - D_n(T)}{\mu_p(T) + \mu_n(T)} \frac{1}{\delta(x,y,z)} \frac{\partial \delta(x,y,z)}{\partial z} \tag{6}$$

The charge carrier conservation equation at the p-n junction is materialized by the following continuity equation [13]

$$\frac{\partial \delta(x,y,z,T,B)}{\partial t} = \frac{1}{e} div(\boldsymbol{J}_n) + G(z) - R(z) \tag{7}$$

The multi-spectral illumination under concentration is given by [9]

$G(z)=C\sum_{i=1}^{3}a_i e^{-b_i z}$ and the recombination rate of the base excess minority carriers is found by [9] $R(z)=\dfrac{\delta(x,y,z,T,B)}{\tau}$. In steady the state, $\dfrac{\partial\delta(x,y,z)}{\partial t}=0$ [13]. According to the study model and in accordance with Equations (1) and (7), the differential equation of continuity of the charge carriers of the PV cell under intense illumination and under variable magnetic field is equal to:

$$C_x\frac{\partial^2\delta(x,y,z,T,B)}{\partial x^2}+C_y\frac{\partial^2\delta(x,y,z,T,B)}{\partial y^2}+\frac{\partial^2\delta(x,y,z,T,B)}{\partial z^2}+\frac{G(z)}{D^*(T,B)}-\frac{\delta(x,y,z,T,B)}{L^{*2}(T,B)}=0 \tag{8}$$

$D^*(B,T)$ and $L^*(B,T)$ are respectively the diffusion coefficient and the diffusion length of the PV cell depending on the variable magnetic field and the temperature: $D^*(B,T)=\dfrac{2D_n\mu_n+D_n\mu_p-\mu_nD_p}{(\mu_p+\mu_n)(1+\mu_n^2B^2)}$ and $L^{*2}(B,T)=D^*(B,T)\cdot\tau$.

Where $C_x=\dfrac{D_n(T)\left[\mu_p(T)+\mu_n(T)\right]}{2D_n(T)\mu_n(T)+D_n(T)\mu_p(T)-\mu_n(T)D_p(T)}$ and $C_y=\dfrac{D_n(T)\left[\mu_p(T)+\mu_n(T)\right]\left[1+\mu_n^2(T)B^2\right]}{2D_n(T)\mu_n(T)+D_n(T)\mu_n(T)-\mu_n(T)D_p(T)}$. The general solution of the Equation (8) is provided by J. Dugas *et al.* as:

$$\delta(x,y,z,B,T)=\sum_j\sum_k Z_{j,k}(z,B,T)\cdot\cos(C_{xj}x)\cdot\cos(C_{yk}y) \tag{9}$$

The resolution of the transcendental equations makes it possible to obtain the values of the coefficients C_j and C_k along the axes (Ox) and (Oy). The expression of the function $Z_{j,k}(z,B,T)$ is obtained by injecting the expression of Equation (9) into the charge carrier continuity equation indicated by Equation (8); this leads to a second order differential equation in $Z_{i,k}$ whose solution is given by:

$$Z_{jk}(z,B,T)=A_{jk}\cosh\left(\frac{z}{L_{jk}(B,T)}\right)+B_{jk}\sinh\left(\frac{z}{L_{jk}(B,T)}\right)-\sum_{i=1}^{3}K_i e^{-b_i z} \tag{10}$$

where $\dfrac{1}{L_{jk}(B,T)}=\left[C_j^2+C_k^2+\dfrac{1}{L^{*2}(B,T)}\right]^{\frac{1}{2}}$,

$K_i=C\dfrac{a_iL_{jk}^2(B,T)}{D_{jk}(B,T)\left[\left(b_iL_{jk}(B,T)\right)^2-1\right]}$ and

$\dfrac{1}{D_{jk}(B,T)}=\dfrac{16\sin\left(C_{xj}\cdot\dfrac{g_x}{2}\right)\cdot\sin\left(C_{yk}\cdot\dfrac{g_y}{2}\right)}{D^*(B,T)\left[\sin(C_{xj}\cdot g_x)+C_{xj}\cdot g_x\right]\left[\sin(C_{yk}\cdot g_y)+C_{yk}\cdot g_y\right]}$. The A_{jk}

and B_{jk} coefficients are determined using the boundary conditions at the junction ($z=0$) and at the rear face of the base ($z=H$) of the PV cell:

$$D^*(B,T)\cdot\left[\frac{\partial\delta(x,y,z,B,T)}{\partial z}\right]_{z=0}=S_f\cdot\delta(x,y,0,B,T) \tag{11}$$

$$D^*(B,T)\cdot\left[\frac{\partial\delta(x,y,z,B,T)}{\partial z}\right]_{z=H}=-S_b\cdot\delta(x,y,H,B,T) \tag{12}$$

2.3. Electrical Parameters

2.3.1. Density of Photocurrent

When the concentrating PV cell is under light incidence, some photogenerated charge carriers cross the junction and produce photocurrent in the external circuit. Thus, from Fick's first law we derive the expression for the photocurrent density, given by the following expression [4]:

$$J_{ph}=\frac{q\cdot D^*(B,T)}{g_x g_y}\int_{-\frac{g_x}{2}}^{\frac{g_x}{2}}\int_{-\frac{g_y}{2}}^{\frac{g_y}{2}}\left[\frac{\partial\delta(x,y,z,B,T)}{\partial z}\right]\mathrm{d}x\mathrm{d}y \tag{13}$$

2.3.2. Photovoltage

The photovoltage characterizes the rate of charge carriers accumulated at the junction of the PV cell. The photovoltage supplied by the solar cell under concentration $C=50$ suns and under an external magnetic field, in 3D, is given by the Boltzmann relation according to the following expression [9]:

$$V_{ph}(B,T)=V_T\ln\left[1+\frac{N_B}{n_i^2}\int_{-\frac{g_x}{2}}^{\frac{g_x}{2}}\int_{-\frac{g_x}{2}}^{\frac{g_x}{2}}\delta(x,y,0,B,T)\mathrm{d}x\mathrm{d}y\right] \tag{14}$$

where $V_T=\dfrac{k_B\cdot T}{q}$ is the thermal voltage; n_i is the intrinsic electron concentration; N_B is the base doping rate.

2.3.3. Electric Power

The electrical power delivered by the PV cell is the product of the photovoltage and the photocurrent depending on the magnetic field and temperature of the base. The expression of the electrical power is given by the following equation [4] [9]:

$$P_{el}(B,T)=J_{ph}(B,T)\cdot V_{ph}(B,T) \tag{15}$$

2.3.4. Conversion Efficiency

The conversion efficiency is the ratio of the maximum power supplied by the PV cell to the incident light power. In this work, the conversion efficiency is a function of the intensity of the magnetic field and the temperature of the base. Thus, the expression of the conversion efficiency is given by [4]:

$$\eta(B,T)=\frac{P_{\max}(B,T)}{P_{inc}} \tag{16}$$

In the case of a concentrated PV cell, the incident power

$P_{inc} = 0.072\ \mathrm{W \cdot cm^2} \times C$. C is the number of suns [14]. Under standard conditions $AM1.5$ and for $C = 50$ suns, $P_{inc} = 3.6\ \mathrm{W \cdot cm^2}$. From the mathematical model and the hypotheses formulated, the expressions of the electrical parameters such as the photocurrent, the photovoltage, the electrical power delivered and the conversion efficiency were established. In the following, it will be a question of presenting the results of the study of the simultaneous influence of the temperature of the base and the magnetic field on the operation.

3. Results and Discussion

3.1. Photocurrent

Figure 2 below shows the behavior of the photocurrent density supplied by the PV cell in an intermediate operating situation.

It appears in Figure 2 that the increase in the intensity of the magnetic field leads to decrease in the photocurrent density. This is explained by the fact that the magnetic field causes a deflection of the charge carriers at due to Lorentz force whose intensity increases with the intensity of the magnetic field. This increase in magnetic field strength the recombination rate of charge carriers in the base and hence a decrease in photocurrent with increasing magnetic field strength [7]. It also appears in this Figure 2 that, for values of the magnetic field B such that $0 < B < 0.4$ mT, the increase in the photocurrent density is accompanied by an increase in the temperature of the base. On the other hand, for values of the magnetic field $B > 0.4$ mT, there is an inversion of the curves, characterized by a drop in the photocurrent with the increase in temperature. Indeed, for $0 < B < 0.4$ mT, the charge carriers diffuse towards the junction and the three phenomena which are thermalization, collisions between charge carriers

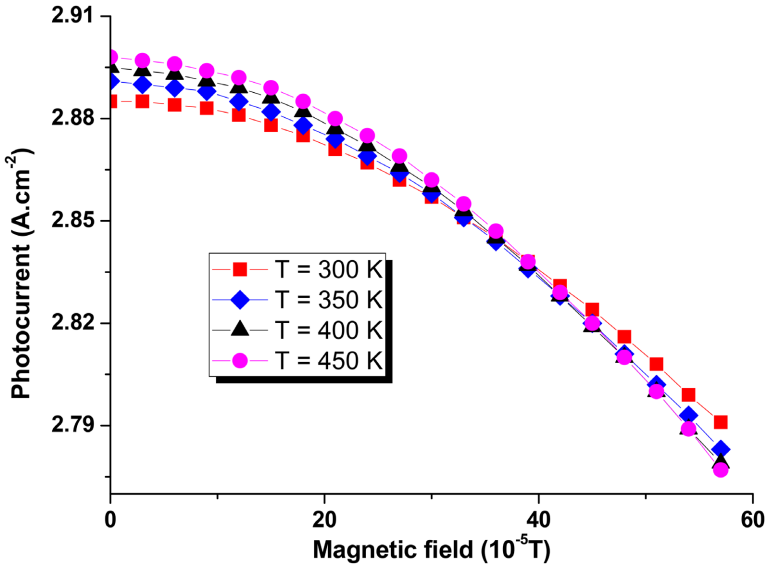

Figure 2. Evolution of the photocurrent versus the temperature of the base and the intensity of the external magnetic field ($C = 50$ suns, $g_x = g_y = 3 \times 10^{-3}$ cm, $S_{gb} = 10^2\ \mathrm{cm \cdot s^{-1}}$, $S_f = 4 \times 10^4\ \mathrm{cm \cdot s^{-1}}$, $S_b = 10^3\ \mathrm{cm \cdot s^{-1}}$).

and braking lead to an increase in the heating of the base. In this case, the increase in photocurrent is accompanied by an increase in temperature. But for the values of the magnetic field $B > 0.4$ mT, the deflection of the carriers becomes important so that fewer carriers diffuse through the junction because of an increase in braking and collisions between charge carriers under the effect of the Lorentz force. There then appears an increase in the energy released in the base and a decrease in the number of charge carriers crossing the junction. This results in the decrease in photocurrent and the increase in temperature for values of $B > 0.4$ mT. Thus, for a given operating temperature, the photocurrent density produced by the PV cell is optimal for low values of the magnetic field intensity.

3.2. Photovoltage

The followings **Figure 3** shows the behavior of the photovoltage supplied by the PV cell, as a function of magnetic field strength, for different values of the temperature of the base.

Figure 3 shows that the photovoltage decreases with the increase in the intensity of the magnetic field, when the PV cell is in an intermediate operating situation. This result is explained by the fact that the increase in the magnetic field leads to increase in the deviations of the charge carriers. Carriers that are deflected to the junction diffuse and those that are deflected to the side surfaces recombine. These two phenomena contribute to a reduction in the density of the carriers in the volume of the base and consequently to a reduction in the photovoltage. It also appears in **Figure 3** that, for magnetic field values such as $0 < B < 0.4$mT, the increase in photovoltage is accompanied by a decrease in temperature. This result is the consequence of the increase in the rate of charge

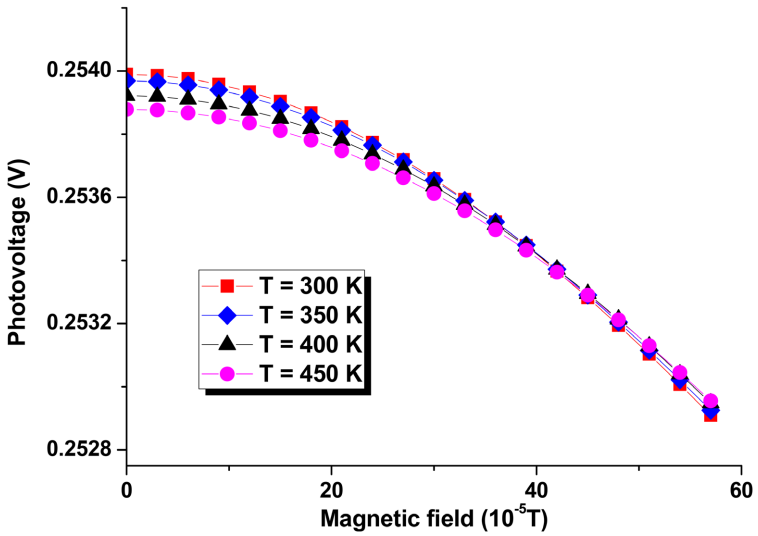

Figure 3. Variations of the photovoltage versus the temperature of the base and the intensity of the external magnetic field ($C = 50$ suns, $g_x = g_y = 3\times10^{-3}$ cm, $S_{gb} = 10^2$ cm·s^{-1}, $S_f = 4\times10^4$ cm·s^{-1}, $S_b = 10^3$ cm·s^{-1}).

carriers blocked in the base. However, the increase in the blocking of carriers in the base causes a reduction in collisions between charge carriers and braking. The energy released in the base decreases and the temperature decreases. On the other hand, for values of the magnetic field $B > 0.4$ mT, there is an inversion of the curves, characterized by an increase in the photovoltage at high temperatures. This result is explained by the fact that at large values of the magnetic field, the deviations become significant and this tends to block the charge carriers in the base. The possibilities of collision between load and braking carriers increase; therefore, the increase in photovoltage is accompanied by an increase in temperature.

3.3. Electric Power

Figure 4 presents the variations in the electrical power delivered as a function of the intensity of the magnetic field for different values of the temperature of the concentration PV cell base.

In Figure 4, it appears that the electric power decreases when the intensity of the magnetic field increases. This result is the consequence of charge carrier deflections with increasing magnetic field strength, which reduces the number of charge carriers that arrive at the junction and the number of charge carriers that diffuse across the junction. As a result, the electrical power decreases with the increase of the magnetic field strength. From below Figure 4, it also emerges that for some given values of the magnetic field induced between 0 and 4×10^{-4} T, the value of the power decreases with the increase in the temperature of the base. In this range of magnetic field values, charge carriers are always oriented towards the junction (but their number decreases with the increase of the magnetic field strength). Then, the energy released in the base by collisions and by

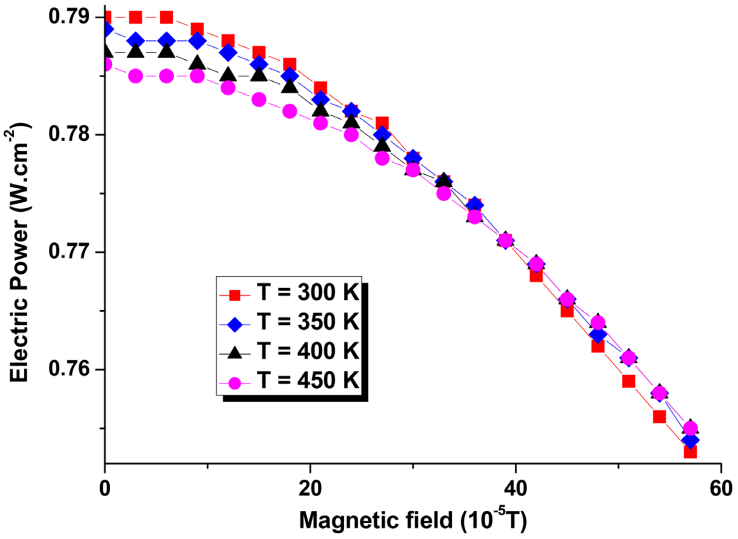

Figure 4. Variations of the electric power according to the temperature of the base and the intensity of the external magnetic field ($C = 50$ suns, $g_x = g_y = 3\times10^{-3}$ cm, $S_{gb} = 10^2$ cm·s^{-1}, $S_f = 4\times10^4$ cm·s^{-1}, $S_b = 10^3$ cm·s^{-1}).

braking increases, which results in an increase in the temperature of the base. For the values of the magnetic field $B > 4\times10^{-4}$ T, we observe an inversion of the phenomenon just like the photocurrent and the photovoltage. Thus, for values of the magnetic field $B > 4\times10^{-4}$ T, a large number of charge carriers are deflected towards the side surfaces and the tendency of the carriers to lock into the base increases. Therefore, there are fewer carriers that are propelled towards the junction because of the deviations and the collisions which increase, but there is an increase in the number of carriers blocked in the base; so that for $B > 4\times10^{-4}$ T, the photocurrent decreases and the photovoltage increases with the temperature of the base, in accordance with Figure 2 and Figure 3 above. The increase in electric power in this case is explained by the fact that when the temperature of the base increases, the gain in voltage is more than the loss in current, so that the electric power increases. This explains the inversion phenomenon for values of the magnetic field $B > 4\times10^{-4}$ T.

3.4. Efficiency

The influence of the intensity of the magnetic field and the temperature of the base on the behaviour of the conversion efficiency is presented in the curves of the following Figure 5.

It appears in Figure 5 that for the values of the magnetic field $B < 4\times10^{-4}$ T, the conversion efficiency decreases when the temperature of the base increases. These results are in good agreement with those of Figure 4 where we observed the drop in the electric power for the same values of the magnetic field B. Indeed, a drop in the delivered electric power leads to a drop in the conversion efficiency. Moreover, for the values of the magnetic field $B > 4\times10^{-4}$ T, there

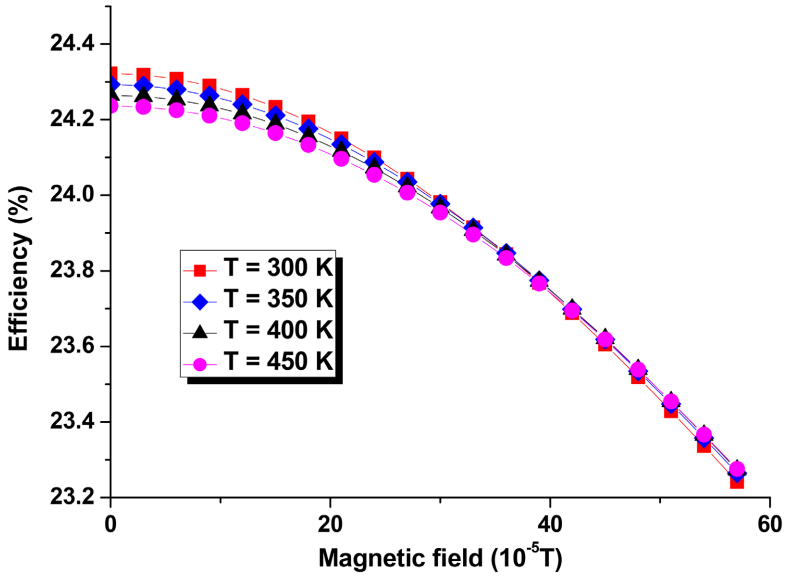

Figure 5. Variations in solar cell conversion efficiency as a function of base temperature and external magnetic field strength ($C = 50$ suns, $g_x = g_y = 3\times10^{-3}$ cm, $S_{gb} = 10^2$ cm·s^{-1}, $S_f = 4\times10^4$ cm·s^{-1}, $S_b = 10^3$ cm·s^{-1}).

appears an inversion of the phenomena, which means an increase in efficiency with the increase in the temperature of the base. These results are also in good agreement with those of **Figure 4** because the conversion efficiency increases when the electrical power delivered increases.

4. Conclusion

This work focused on the study in three dimensions (3D) of the behaviour of the electrical parameters according to the temperature of the base and an external magnetic field, of a PV cell under concentration of 50 suns. It appears from this study that the rise in temperature on the one hand and on the other hand the increase in the intensity of the magnetic field causes a drop in the performance of the PV cell, which is in good agreement with the work of other authors. However, the study of the simultaneous effects of temperature and magnetic field reveals an unexpected phenomenon. Indeed, an inversion of the curves is observed for the values of the magnetic field $B > 4\times10^{-4}$ T. This result reflects the fact that for values of the magnetic field $B > 4\times10^{-4}$ T, the performance of the PV cell is slightly improved for high base temperatures.

Acknowledgements

The authors are thankful to International Science Program (ISP) which is supporting our research group (energy and environment) and allowing the conduct of our works.

Conflicts of Interest

The authors declare no conflicts of interest regarding the publication of this paper.

References

[1] Ouedraogo, A., Mogmenga, L., Bado, N., Ky, T.S.M. and Bathiebo, D.J. (2020) Analysis of the Single-Crystalline Silicon Photovoltaic (PV) Module Performances under Low γ-Radiation from Radioactive Source. *Silicon*, **12**, 1831-1837. https://doi.org/10.1007/s12633-019-00282-7

[2] Ouédraogo, A., Zouma, B., Ouédraogo, E., Guissou, L. and Bathiébo, D.J. (2021) Individual Efficiencies of a Polycrystalline Silicon PV Cell versus Temperature. *Results in Optics*, **4**, 100101. https://doi.org/10.1016/j.rio.2021.100101

[3] Green, M.A., Dunlop, E.D., Siefer, G., Yoshita, M., Kopidakis, N., Bothe, K. and Hao, X.J. (2023) Solar Cell Efficiency Tables (Version 61). *Progress in Photovoltaics: Research and Applications*, **31**, 3-16. https://doi.org/10.1002/pip.3646

[4] Soro, B., Savadogo, M., Zouma, B., Tchedre, K.E., Sourabié, I., Zerbo, I., Zoungrana, M. and Bathiebo, D.J. (2021) 3-D Modelling of Electrical Parameters' Effects on the Heating of the Base of an Intense Light Illuminated Polycrystalline Silicon PV Cell. *Journal of Fundamental and Applied Sciences*, **13**, 1380-1388. https://doi.org/10.4314/jfas.v13i3.15

[5] Soro, B., Zoungrana, M., Zerbo, I., Savadogo, M. and Bathiebo, D.J. (2017) 3-D Modeling of Temperature Effect on a Polycrystalline Silicon Solar Cell under In-

tense Light Illumination. *Smart Grid and Renewable Energy*, **8**, 291-304. https://doi.org/10.4236/sgre.2017.89019

[6] Toure, F., Zoungrana, M., Zouma, B., Mbodji, S., Gueye, S., Diao, A. and Sissoko, G. (2012) Influence of Magnetic Field on Electrical Model and Electrical Parameters of a Solar Cell under Intense Multispectral Illumination. *International Journal of Advances in Science and Technology*, **5**, 40-53.

[7] Soro, B., Savadogo, M., Tiendrebéogo, S., Bathiébo, D.J., Zoungrana, M. and Zerbo, I. (2017) The Effect of Magnetic Field on the Efficiency of the Silicon Solar Cell under an Intense Light Concentration. *Advances in Science and Technologie Reseach Journal*, **11**, 133-138.

[8] Zoungrana, M., Zerbo, I., Ouédraogo, F., Zouma, B. and Zougmoré, F. (2012) 3D Modelling of Magnetic Field and Light Concentration Effects on a Bifacial Silicon Solar Cell Illuminated by Its Rear Side. *IOP Conference Series: Materials Science and Engineering*, **29**, 012020. https://doi.org/10.1088/1757-899X/29/1/012020

[9] Barro, F.I., Sam, R., Touré, F., Samb, M.L., Zoungrana, M., Zerbo, I. and Zougmoré, F. (2011) Modélisation à 3-d de l'influence de la taille des grains et de la vitesse de recombinaison aux joints de grain sur une photopile au silicium polycristallin sous éclairement concentrée. *Revues des Energies Renouvelables*, **14**, 649-664.

[10] Mbodji, S., Gueye, S., Dieng, M., Sissoko, G., Samb, M.L. and Sarr, S. (2009) Etude en modélisation à 3-d d'une photopile au silcium en régime statique sous éclairement multispectral: Détermination des paramètres électriques. *Journal of Science*, **9**, 36-50.

[11] Sudre, C., Pelanchon, F. and Moreau, Y. (1992) Solar Cell under Intense Light Concentration: Numerical and Analytical Approaches. 11*th European Photovoltaic Solar Energy Conférence*, Montreux, Suisse, 12-16 October, 1992.

[12] Betser, Y., Ritter, D., Bahir, G., Cohen, S. and Sperling, J. (1995) Measurement of the Minoritory Carrer Mobility in the Base of Heterojunction Bipolar Transistor Using a Magneto-Transport Method. *Applied Physics Letters*, **67**, 1883-1884. https://doi.org/10.1063/1.114364

[13] Mathieu, H. (2009) Physique des semi-conducteurs et de quelques composants électroniques. DUNOD, Paris.

[14] Equer, B. (1993) Energie solaire photovoltaïque: Physique et technologie de la conversion photovoltaïque. CNRS France, Volume 1, Ellipses, Paris.